

# Coupled Electromagnetic, Structural-Dynamic, and Acoustic Simulation of an Induction Furnace

Dirk van Riesen and Kay Hameyer

Institute of Electrical Machines, RWTH Aachen University, D-52062 Aachen, Germany

Induction furnaces for melting metals are well understood and optimized electromagnetically. New challenges arise, however, when regarding the whole device. Especially the vibrations and the acoustic noise are of importance, as the frequency of operation and the rated power of the devices are rising quickly. Since the vibrations are a result of the electromagnetic forces, a coupled simulation is required that regards all relevant effects. In this paper, the methods for the electromagnetic, structural-dynamic and acoustic simulations are presented as well as the coupling procedures. In the structural-dynamic part, a fluid-structure-interaction is used to regard the effect of the liquid melt.

*Index Terms*—Acoustics, coupled simulation, FEM, induction furnace, vibration.

## I. INTRODUCTION

INDUCTION furnaces are, from the electromagnetic point of view, rather simple devices. Fig. 1(a) shows the principle of operation. An outer coil is driven with a sinusoidal current. The magnetic field produced penetrates the melt, which acts as a short-circuited secondary coil. Eddy currents produce losses, which then heat up the melt. The magnetic field, together with the currents, both in the coil and the melt, produces Lorentz forces. The constant component produces a material flow in the melt, while the alternating component produces vibrations of the structure.

Fig. 1(b) shows the geometry of an induction furnace. Advances in power electronics have permitted to raise the power and the operating frequency. Power supply frequency (50–60 Hz) devices are replaced by mid-frequency (250 Hz) furnaces, which allow for higher power induced in the melt and thus reduced melting times. The regarded furnace is designed to melt 6 tons of gray cast iron, with a rated power of 4.5 MW. The coil current is 18 kA with a rated frequency of 250 Hz. These high currents produce also very high Lorentz forces. The vibrations can no longer be neglected. In combination with the raised frequency (500 Hz, twice the electric frequency), the acoustic noise produced must be regarded as well. Such large and cost-intensive devices cannot be analyzed and optimized with prototypes. Therefore, a simulation method regarding the electromagnetic fields, the structural-dynamic vibrations and the acoustic noise is needed. This paper presents the three simulations and the coupling between them.

## II. ELECTROMAGNETIC SIMULATION

The furnace is driven with a single-frequency sinusoidal current. Due to the construction, large air gaps are present. Thus, no saturation takes place. The electromagnetic simulation uses a time-harmonic formulation with linear material properties. The magnetic vector potential  $\vec{A}$  and the electric vector potential  $\vec{T}$  are coupled to take into account eddy-current effects. The

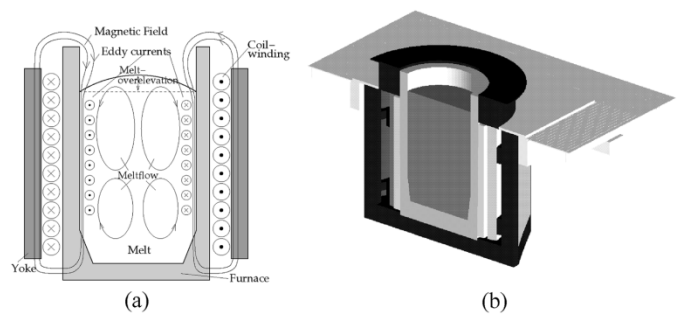


Fig. 1. Induction furnace. (a) Principle of operation. (b) Geometry.

formulation for nonconducting regions in Galerkin formulation reads

$$\int_{\Omega} (\nabla \times \vec{\alpha}_i \cdot \nu \nabla \times \vec{A}_i) d\Omega = \int_{\Omega} (\vec{\alpha}_i \cdot \vec{J}_0) d\Omega \quad (1)$$

$$\forall i = 1, 2, \dots, n_e. \quad (2)$$

Edge elements are used. In the eddy-current regions the formulation reads (in Galerkin form)

$$\int_{\Omega_c} (\nabla \times \vec{\alpha}_i \cdot \nu \nabla \times \vec{A}_i - \vec{\alpha}_i \cdot \nabla \times \vec{T}) d\Omega = 0 \quad \forall i = 1, 2, \dots, n_e$$

$$\int_{\Omega_c} \left( \nabla \times \vec{\alpha}_i \cdot \frac{1}{\sigma} \nabla \times \vec{T} + \nabla \times \vec{\alpha}_i \cdot j\omega \vec{A} \right) d\Omega = 0 \quad \forall i = 1, 2, \dots, n_e.$$

Different combinations of magnetic and electric potentials are possible [1], [2]. The chosen formulation allows for current driven eddy current regions, which is needed when regarding the coil windings. Since they are built as water cooled solid copper conductors, the eddy currents can not be neglected there. Source currents are impressed as boundary conditions for the electric vector potential  $\vec{T}$ . Fig. 2 shows the flux density, the current density and the resulting Lorentz forces for one winding. The convergence of this formulation is not as stable as others for higher frequencies [3], but at the regarded frequencies between 50 and 250 Hz it is not yet a problem [4]. Fig. 3 shows the convergence of the CG algorithm for different frequencies.

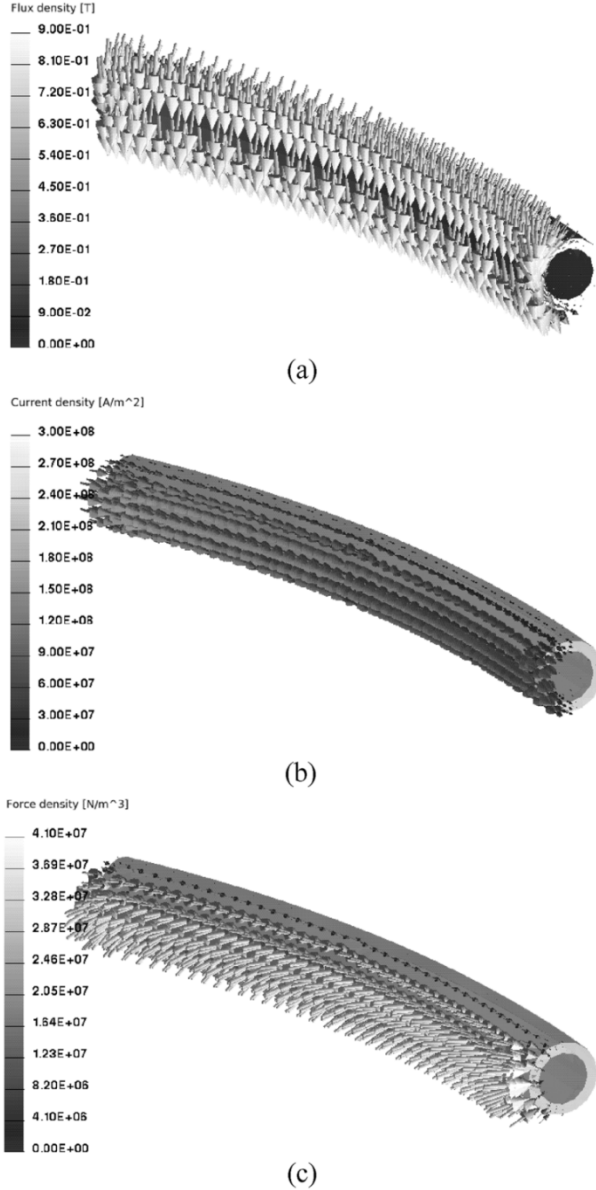


Fig. 2. Flux density, (a) current density, (b) and resulting Lorentz force, (c) for one coil winding.

The electromagnetic simulation is implemented in the open-source software iMOOSE [5].

### III. STRUCTURAL-DYNAMIC SIMULATION

The Lorentz forces resulting from the electromagnetic simulation are transformed to a structural-dynamic model. This model has to take into account constructive details. The symmetry is not as pronounced as in the electromagnetic case. Therefore, a 180° model is used (Fig. 4). Hexahedral elements are used due to their higher accuracy for structural-dynamic simulations.

The Lorentz force density resulting from the electromagnetic simulation is transformed to nodal forces on the structural-dynamic model, like shown in Fig. 5. The transformation from the 30° model to the 180° is accomplished by rotating and mirroring of the forces.

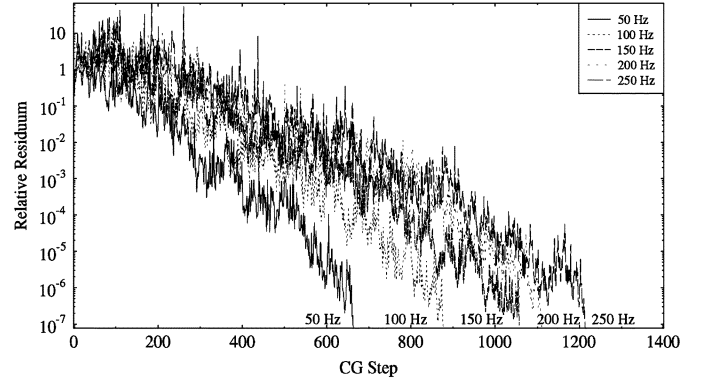


Fig. 3. Convergence of the CG algorithm for different frequencies.

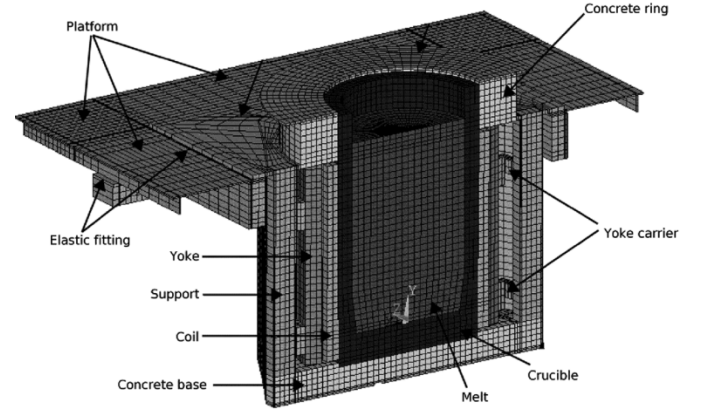


Fig. 4. Structural-dynamic model.

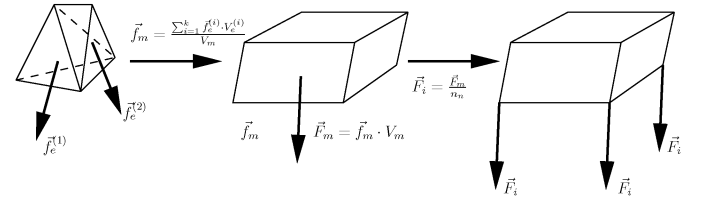


Fig. 5. Force transformation.

The equation to be solved reads

$$(\mathbf{K} + j\Omega\mathbf{C} - \Omega^2\mathbf{M}) \cdot \mathbf{D} = \mathbf{F} \quad (3)$$

A time-harmonic approach is used. This equation can be solved either directly using a CG algorithm for a given frequency  $\Omega$  and a given force excitation  $\mathbf{F}$ , or using a numerical modal analysis. Since the induction furnace is driven at varying frequencies between 50 and 250 Hz depending on the fill level of the melt, it is important to regard a wider frequency range. After solving the generalized eigenvalue problem

$$(\mathbf{K} - \omega_i^2\mathbf{M}) \Phi_i = 0 \quad (4)$$

the eigenvalues  $\omega_i$  and eigenvectors  $\Phi_i$  are obtained and arranged into matrices

$$\Phi = (\Phi_1 \dots \Phi_n)$$

and

$$\omega^2 = \text{diag} [\omega_i^2], \quad i = 1, 2, \dots, n_m. \quad (5)$$

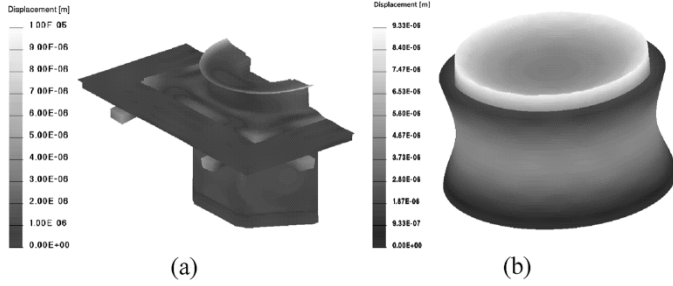


Fig. 6. Deformation of the structure (a) and the melt (b) at 470 Hz. (a) Deformation at 470 Hz. (b) Deformation of the melt.

With this, the displacement of the nodes in the structural-dynamic model can be computed for a given frequency and force excitation directly, without the need of an iterative solution

$$\underline{D}_i = \sum_{j=1}^{n_m} \sum_{k=1}^{n_m} \Phi_{ij} \Phi_{kj} \frac{F_k}{-\Omega^2 + j2\xi_j \Omega \omega_j + \omega_j^2}. \quad (6)$$

$\xi_j$  is the damping factor for the  $j$ -eigenfrequency.

The melt is regarded either as mass elements on the crucible or with a fluid-structure interaction. The latter allows to compute the vibrations on the free surface of the melt, to take into account also the acoustic noise produced there. The structural-dynamic simulation is performed using the software Ansys [6]. Fig. 6(a) shows a deformation plot at 480 Hz, while Fig. 6(b) shows the deformation of the melt simulated with the fluid-structure interaction.

The result, shown as deformation plots (cf. Fig. 6) is not the best possibility to compare or evaluate different solutions. Therefore, an integral quantity is introduced. It is based on the transfer function of one node  $h_{ik}$  [7]. It shows the amplitude of deformation of the node  $i$  as result of a force  $F_k$  acting on another node  $k$

$$h_{ik} = \frac{D_i}{F_k}. \quad (7)$$

For the body sound level the velocity inside an element is described as the derivative of the transfer function [8] and the body sound level is built as

$$L_S(\Omega, m) = 10 \log \left( \frac{\Omega^2 \sum_{p=1}^{N_{el}} \int_{S_p} |\mathbf{N}^p \mathbf{h}_p^m(\Omega) \cdot \mathbf{n}^p|^2 dS}{S_0 h_{U_0}^2} \right) \quad (8)$$

$\mathbf{n}^p$  is the normal to the element  $p$ ,  $\Omega$  the frequency.  $m$  refers to the node, where the force is acting.  $S_0 h_{U_0}^2$  are reference quantities from literature ( $S_0 = 1 \text{ m}^2$ ,  $h_{U_0}^2 = 25 \cdot 10^{-16} \text{ m}^2 / (\text{s}^2 \text{ N}^2)$ ). For the induction furnace a variant is used. The body sound level is built not on basis of the transfer function, but instead the velocity resulting from the total acting forces is taken. Therefore, the magnitude of the excitation is also regarded in the resulting level:

$$L_S(\Omega) = 10 \log \left( \frac{\sum_{p=1}^{N_{el}} \int_{S_p} |v_p \cdot \mathbf{n}^p|^2 dS}{S_0 h_{U_0}^2} \right). \quad (9)$$

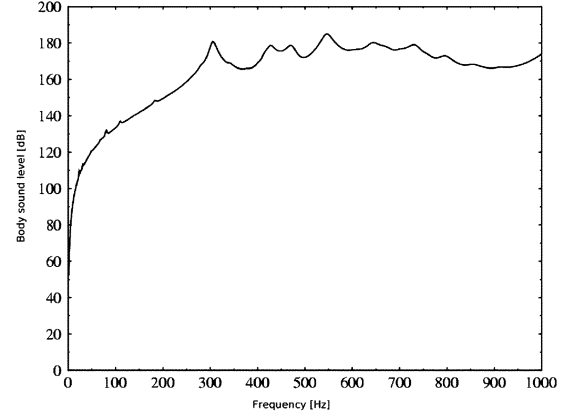


Fig. 7. Modified body sound level of the induction furnace.

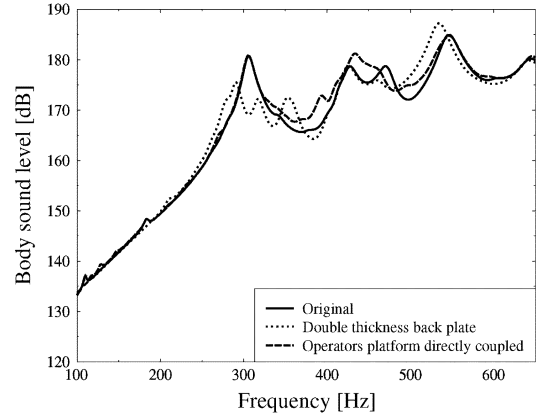


Fig. 8. Modified body sound level of construction variants.

The same reference quantity as above is used, but with a different unit ( $h_{U_0}^2 = 25 \cdot 10^{-16} \text{ m}^2 / (\text{s}^2)$ ). This results in values that are higher than expected, but they are only used for comparison between different variants.

Fig. 7 shows the body sound level as a result of maintaining a constant force excitation over a frequency range of 0 Hz to 1 kHz.

With this integral quantity, variations in the construction of the device can be evaluated with respect to their impact on the vibration. Fig. 8 shows the effect of doubling the thickness of the back plates and coupling the operators platform directly to the supporting structure without rubber elements.

Measuring the vibrations of the induction furnace during the operation is not easily possible, due to the high temperatures, dirt, and the operation of the device. It is not possible to operate in a stationary operating point, as the metal would overheat. Thus, a melting cycle of about 45 min. for 6 tons of gray cast iron is characterized by varying frequencies and currents. Nevertheless, it is possible to perform an experimental modal analysis of different parts of the cold induction furnace. Fig. 9 shows the mean acceleration values for the back cover plate as an example. Comparing this to the acceleration resulting from the numerical simulation, it can be found, that the agreement in respect to the frequency response is good. The amplitudes cannot be compared, since the force excitation in both cases is

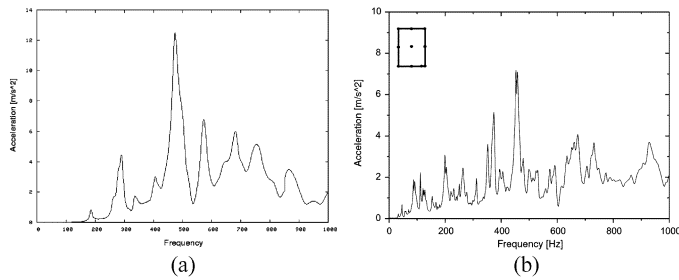


Fig. 9. Simulated and measured accelerations of the back cover plate. (a) Simulated. (b) Measured.

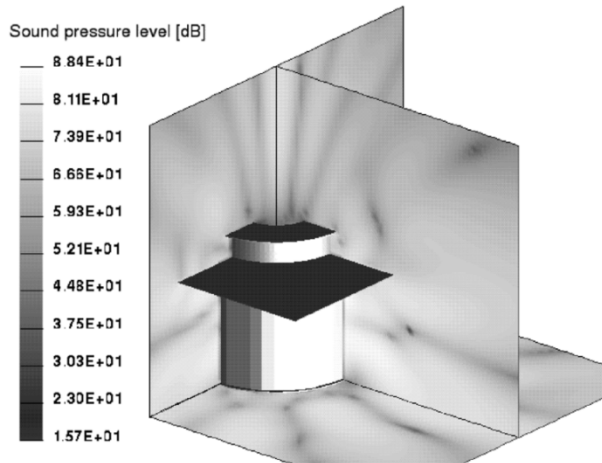


Fig. 10. Sound pressure level distribution around the induction furnace.

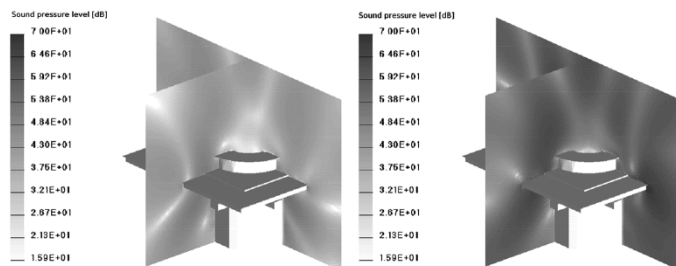


Fig. 11. Sound pressure level as result from different constructive measures.

different. Comparing the vibration modes of the structure between the experimental modal analysis and the simulation, a good agreement is found as well.

#### IV. ACOUSTIC SIMULATION

The displacement values of the structure obtained from the structural-dynamic simulation are transferred to another FE model of the induction furnace. This is a surface model, representing the outer surfaces of the device. Triangular elements are used. The coupling of the models is performed via a geometrical search algorithm. The acoustic noise emanating from the structure is computed using a boundary element solver [9].

Fig. 10 shows the sound pressure distribution computed on areas around the furnace. The distribution and amplitude can be used to evaluate the effect of different constructive measures. Fig. 11 shows the sound pressure level distribution for the

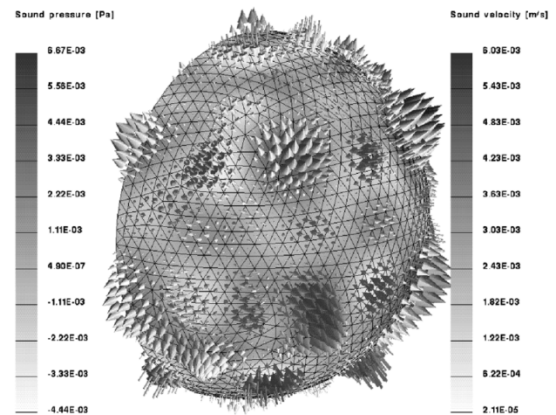


Fig. 12. Acoustic power calculation on a spherical integration surface.

variants also depicted in the structural-dynamic simulation section, doubling the thickness of the back plate and directly coupling the operator's platform to the supporting structure without rubber elements. It can be seen that specially this measure leads to a higher sound output, as expected.

Alternatively, the acoustic power is used as an integral quantity for comparison.

#### V. CONCLUSION

The electromagnetic, structural-dynamic and acoustic simulation of an induction furnace using coupled FE methods has been presented. The weak coupling between the three simulation methods allows to compute the acoustic noise produced by electromagnetic excitation. Integral quantities are introduced to evaluate and compare the results of different construction variations.

#### REFERENCES

- [1] O. Bíró, "Edge element formulations of eddy current problems," *Comput. Methods Appl. Mech. Eng.*, vol. 169, pp. 391–405, 1999.
- [2] D. van Riesen, C. Kaehler, and G. Henneberger, "Convergence behavior of different formulations for time-harmonic and transient eddy-current computations in 3d," *IEE Proc. Sci., Meas. Technol.*, to be published.
- [3] C. Kaehler, D. van Riesen, D. Albertz, and G. Henneberger, "Comparison of the  $\vec{A} - \vec{A}, \vec{T}$  and the  $\vec{A}$ -formulation for the computation of transient eddy-current field problems with edge elements," in *Proc. IGTE'02*, Graz, Austria, 2002, p. 88.
- [4] D. van Riesen, C. Kaehler, and G. Henneberger, "Comparison of different formulations for eddy-current computations in an induction furnace," in *Extended Papers—PIERS, Progress in Electromagnetic Research Symp.*, Mar. 2004, pp. 623–626.
- [5] G. Arians, T. Bauer, C. Kaehler, W. Mai, C. Monzel, D. van Riesen, and C. Schlenk. *Innovative Modern Object-Oriented Solving Environment—iMOOSE*. [Online]. Available: <http://www.imoose.de>
- [6] Ansys [Online]. Available: <http://www.ansys.com>
- [7] F. G. Kollmann, *Maschinenakustik: Grundlagen, Messtechnik, Berechnung, Beeinflussung*, 2nd ed. Berlin, Germany: Springer, 2000.
- [8] F. Hibinger, "Numerische Strukturoptimierung in der Maschinenakustik," Ph.D. dissertation, Darmstadt, 1998. TU Darmstadt.
- [9] T. Bauer, C. Monzel, and G. Henneberger, "Three-dimensional calculation of the acoustic behavior of electrical machines using boundary element method," in *Proc. Int. Seminar on Vibrations and Acoustic Noise of Electric Machinery*, Béthune, France, May 1998, pp. 69–73.